

WINDTHROW DETECTION BY SATELLITE IMAGES AND EFFECT ASSESMENT

Paula Furtună¹, N. Maier², I.H. Holobacă¹

Key words: windthrow detection, satellite images, GIS, meteorological risk.

Abstract. The windthrow detection, meteorological risk factor, based on satellite imagery and the assessment of their effects. Windthrow detection has always been and still represents a problem on an economical and ecological level because of the national negative effects they have. (Popa, I., 2000). Therefore, the detection and quantitative evaluation of woody debris constitutes one of the major applications of remote sensing in the management of environmental resources and in the decision to rehabilitate natural landscapes. The paper presents the results of the research on detection of wind caused debris with the help of satellite images, and the meteorological causes that brought about the phenomenon. The meteorological analysis was made with the help of data from the Doppler radars WSR-98D from Bobohalma, showing descendent movements of convective origin. The geographical analysis allowed the highlighting of the affected areas, the most affected being the slopes with north, north-west and north-east exposure, having an inclination of >14 and situated between 1250m-1400m altitude with a surface of up to 5ha.

Introduction

The windthrow term stands for any mechanical damage which affects a tree or brush as a result of the wind. The observation of the main aspects concerning the mechanism that causes the mechanical damage of the forest ecosystem as a result of the disruptive action of the wind is facilitated by the systematization of the windthrow into two categories: windthrow with catastrophic effects (catastrophic windthrow) and endemic windthrow, the criteria of classification being the intensity and magnitude of the phenomenon reported to a certain geographical scale of analysis (Popa, 2005).

For the analysis and knowledge of the present state of the problem of windthrow, an ample documentation has been done by using various sources:

¹ Babeş-Bolyai University, Faculty of Geography, 5-7, Clinicilor Street, Cluj-Napoca, 400006, Cluj County, Romania, paula_roxana.furtuna@yahoo.com , holobaca@ubbcluj.geografie.ro

² National Meteorological Administration, Regional Meteorological Center Transilvania Nord, 17, Vânătorului Street, Cluj-Napoca,400213, Cluj County, România, mcis73@yahoo.com

specialized journals, PhD thesis, research reports and various documents. It was noted that *the first time interest was shown in the subject dates back to the 16th century* (Pauna, A., 2011) when foresters started paying more and more attention to the calamities caused by strong winds or heavy wet snows.

As a meteorological risk, windthrows are characterized by temporary, instantaneous appearance, depending on the speed of the wind which can be over 15-25-50m/s, the short duration (from a few hours up to 24 hours), the large amplitude in the field (from isolated trees to tens or hundreds of hectares), as well as the unpredictable economical and ecological consequences, the most vulnerable being the forest ecosystems situated on the slopes under the wind, crossed by warm or cold catabatic winds (such as the Foehn or the Bora) (Bogdan, Octavia, 2010)

1. Data sources and methods used

1.1 Studied area. Keeping in mind the complexity of the studied phenomenon and the objectives, the test area UP IV Canciu from Ocolul Silvic Cugir was selected, subordinated to the Forestry Department Alba, which was affected by wind caused debris in June 2007 (figure 2.1).

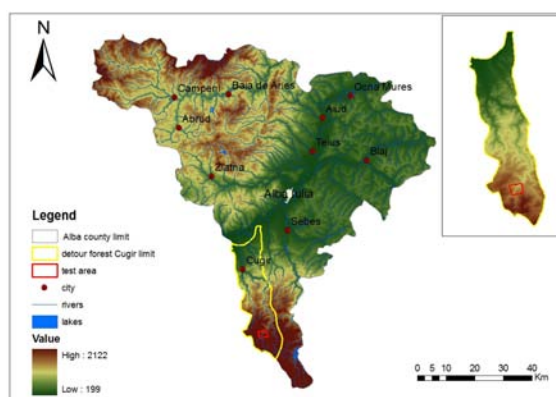


Fig.1.2. Location of District Forest Cugir

The forests administered by District Forest Cugir, with a surface of 19086.5ha, are situated in the central part of the country, more specifically in the south-western limit of Alba County (according tot Forest management of District Cugir, 2003). The forests are located in the basins of the rivers Mare and Mic, tributaries to Cugir. The division of the area is in 6 production units, numbered from UP I to UP VI as follows: Saliste, Cugir, River Mare, Canciu, Lupsa, River Mic.

The general aspect is determined by the Râul Mare and Mic, which flow from south to north, therefore having a general northern exposure. The hydrographic network is rich enough, and the fragmentation of the land gives rise to the complete range of exposures.

1.2 Data sources and methodology. A set of Landsat 7 ETM images (with 7 spectral bands and 30 m spatial resolution) from various dates were used: 10th October 2006, before the windthrow occurred, and 20th July 2007, right after it occurred. The Landsat images were downloaded free of charge from the site <http://glovis.usgs.gov/>.

The Aster Gdem digital terrain's model was also used (<http://www.jspacesystems.or.jp/ersdac/GDEM/E/index.html>), at a 30m resolution.

The synoptic analysis was made on the grounds of the data received from the Doppler radars WSR-98D from Bobohalma, Mures county. To calculate the speed of the wind bursts the corresponding values of VIL and ET were used and applied in the formula which was also used by researchers from Air Force's Air weather service 1996.

$$W = [(15,780608 \cdot \text{VIL}) - (2,3810964 \cdot 10^{-6} \cdot \text{ET}^2)]^{1/2} \text{ (AWS, 1996)}$$

Where: VIL is the water volume from the column, [$\text{kg} \cdot \text{m}^{-2}$], ET is the height of the cloud (echo) [km].

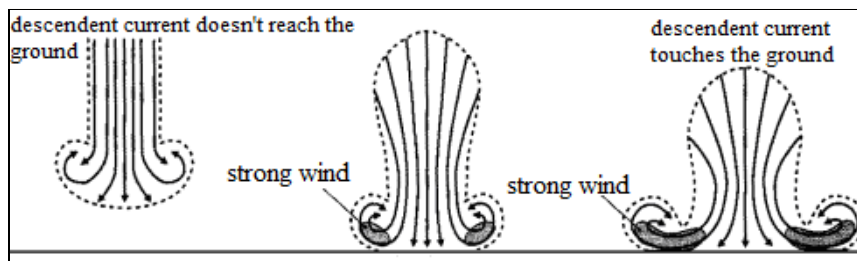


Fig. 2.1. Conceptual model of convective wind formation (Wakimoto 2001)

Windthrow detection was done by comparing the two satellite images prior and after the event. In figure 2.2 are presented the two above mentioned images, the visual analysis highlighting the affected areas.

To highlight the areas affected by the windthrow, several principles were applied. First the satellite index NDVI (Normalized Difference Vegetation Index) for the images taken in 2006 and 2007 were calculated, then the rapport and subtraction between them was made.

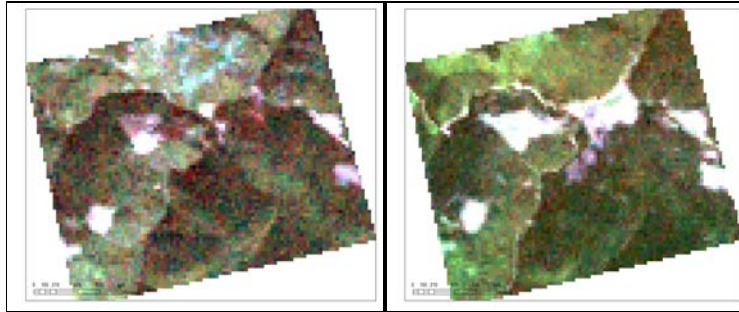


Fig. 2.2 Composite Landsat TM image 321 color in 2006 (a) and 2007 (b), (the area affected by windthrow is colored in white)

NDVI is defined as the rapport between the subtraction of the infrared-red bands, and the sum of the two respectively.

$$NDVI = (NIR-R) / (NIR+R) = (Band\ TM\ 4 - Band\ TM\ 3) / (Band\ TM\ 4 + Band\ TM\ 3),$$

Where:

NDVI – normalized difference vegetation index

NIR – Near Infra Red Band – band 4 Landsat TM și ETM+

R – Red spectral band (visible, Red-band 3 Landsat Tm and ETM+)

The interpretation implies the delimitation of the areas in tones of different colors, which obviously shows characteristics of the vegetation.

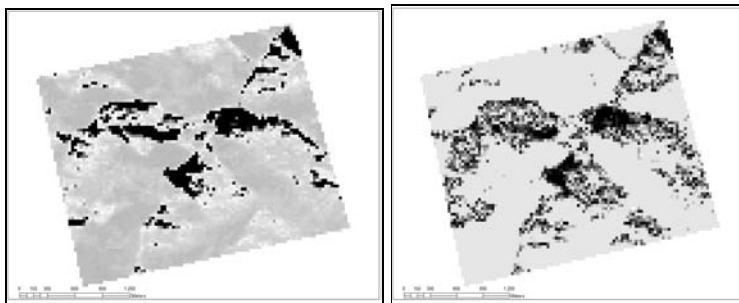


Fig. 2.3 Land cover change detection using NDVI as input: a-by difference, b- by report

The highest values of NDVI are correspondent to the tones of white, and reaches up to 1, these are associated with the thickest and healthiest forests.

The darkest tones, close to black, show the exact opposite of what was mentioned above. The lack of vegetation, of chlorophyll, is expressed by the bare soil, or rock, which absorb the near infrared more.

The medium values are in tones of lighter or darker grey. They can be associated to the broadleaf forest and coniferous forest when the tones are of light-grey, the darker-grey showing inconsistent grassland which does not cover everything.

In the figure 2.3 the subtraction and the rapport for NDVI of the two images are presented (from 2006 and 2007).

In order to facilitate the visual analysis as well as for determining the precise extension of the affected areas, the progressive slicing of density was used. That allowed the changing of the color of the pixels up until the selected pixels covered and highlighted the affected area.

Another method used was the method of principal components analysis (PCA).

The implementation of the principal components analysis was used with the purpose of obtaining images which would be easier to interpret and more suggestive, and that would be able to provide the highest amount of information possible. At the same time the PCA allowed getting improved images from a spectral point of view.

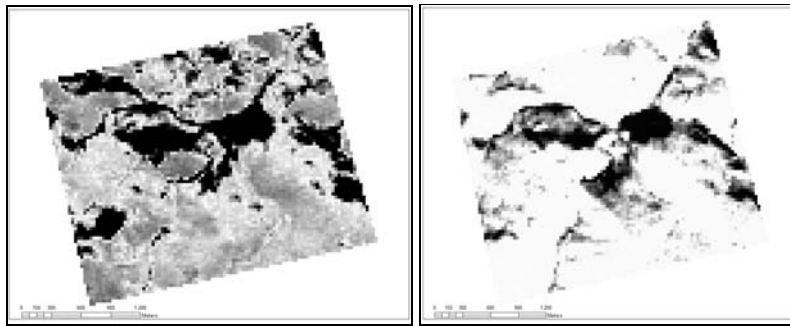


Fig. 2.4. Land cover change detection using as input to PC1: a-by difference and b- by report

In the fig. 2.4 are presented in comparison the subtraction and rapport for PC1 of the two images, and after the visual analysis, it was determined that there are no significant differences between the subtraction method and the rapport method between the pixel values from the two images. The maximum consistency of the vegetation is shown by the high value represented by the tones of white, and the debris is represented by the color black.

Just like in the case of NDVI, the slicing of progressive density was carried out, hence better showing the area affected by the windthrow.

The next stage implies the recording of the PC1 image, which is a raster map in only two values: 0 – for the areas that do not show any changes, do not show the effect of windthrow, and 1 – for areas that show windthrow. Then the raster map was “flattened” by the application of the “Majority” function, the result being presented in figure 2.5 (a).

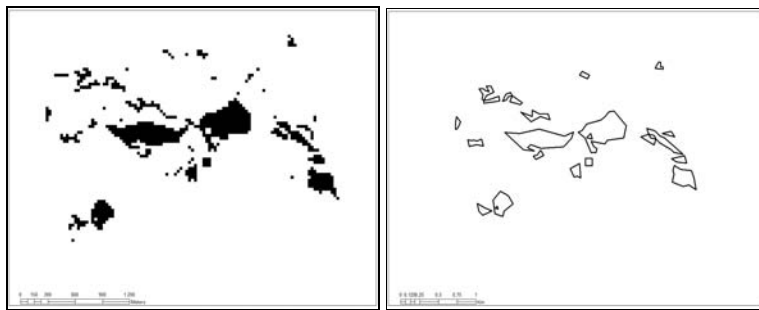


Fig. 2.5. "The flattened" with "Majority" of 1-bit raster map, - (a) polygon vector layer obtained by changing the representation of raster to vector representation,-(b).

For the geo-spatial analysis a switch from the raster representation mode to the vector representation was made. The result is a polygon type ground, presented in figure 2.5 (b). In this way the vector limit of the polygons was marked at the limit between pixels with different values (in this case with values 0 and 1).

2. Results and discussion

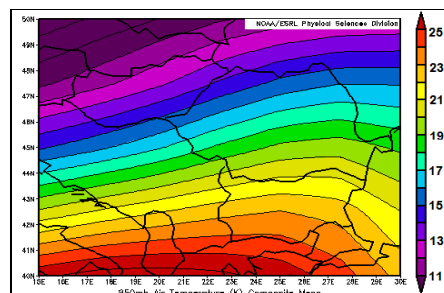


Figure 3.1. The structure of air temperature at 850 hPa level (processing by <http://www.esrl.noaa.gov>) the day 23.06.2007

a. Analysis of the meteorological causes which generate debris. During the time that the windthrow took place in 2007, Romania was under the influence of the western air masses, characterized by high humidity, rich rainfall and western winds, and temperatures between 15°C and 23°C, (figure 3.1).

The windthrow was caused by descending movements of convective origin, which are associated with the development of cumulus clouds and storms.

At ground level this descending current becomes a surface wind on the direction of the general current, or channeled by the relief.

This wind is known as the first burst. In areas with higher relief the descending current tends to move on through the main drainage net. Speeds of 15 on 25 $\text{m}\cdot\text{s}^{-1}$ are frequent for these gusts. High speeds and surface roughness contact can cause very strong winds. They are all the stronger the more the air mass is warmer. Although convective winds occur suddenly and violently, are of short duration. Winds descendents are characteristic for mature storms, but for their occurrence is not necessary achieving stage of maturity.

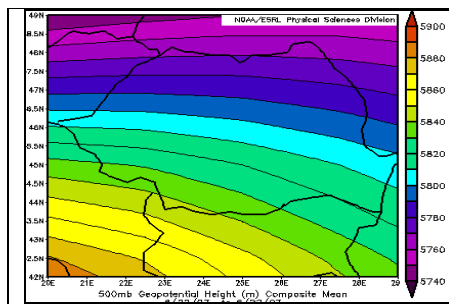


Figure 3.2 Geopotential field at 550hPa (5500 m), 23.06.2007

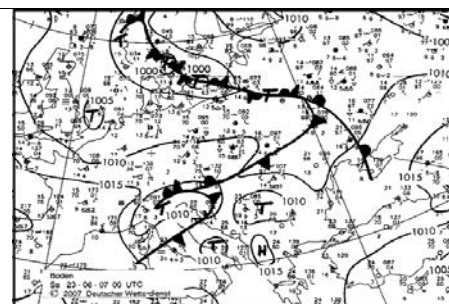


Figure 3.3. The ground-level pressure , 23.06.2007

The configuration of field geo-potential at the level of 500hPa puts our country on the ascending side of the flux, in an area of parting isohypses (figure 3.2). The geo-potential value was low, having values of under 5790 m, being relatively steady.

The center of Europe is under the influence of a field of low pressure. In the north of Italy there is a Mediterranean cyclone evolving, which brought an input of warm and humid air, and in the center of Poland, a cyclone of Icelandic origin with a relatively cold air mass. At ground level a front end corridor can be observed, which passes through Romania on the night of the 22nd to 23rd of June 2007 (figure 3.3).

The above figures show how the wind bursts started on the 22nd of June, at 3:00 and are concentrated on the south of the OS Cugir where the testing area is situated, having a speed of 23m/s but lose their intensity once they start moving east, (because of a technical difficulty of the radar, not all the data from that day is available) (figure 3.4).

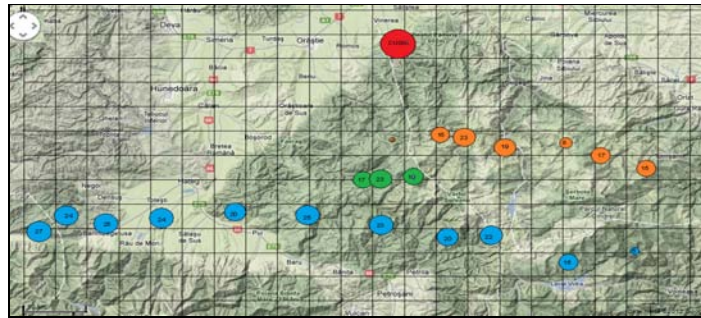


Fig. 3.4 Gusts speed during 22 to 23 June 2007 superimposed over the affected area

During the 23rd June the wind bursts started at about 4:00 and had a west-east orientation, passed through the testing area with a speed of 27m/s; at 4:13 they were situated above the testing area having a speed of 23m/s, and after that it began decreasing in intensity while moving east.

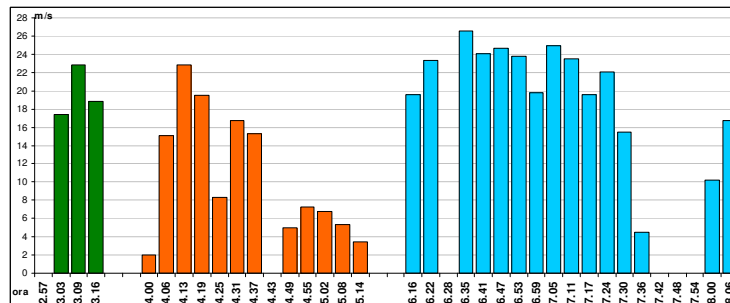


Fig. 3.5 Gust speed and times began

The same day, at 6:16 a new wind burst took place to the south of the testing area, which had the maximum speed of 25m/s and which lost from its intensity while moving east. All these descending movements of convective origin were concentrated on the valleys and knocked down trees.

b. The analysis of the windthrow. This methodology for detecting and evaluating the areas affected by windthrow is a clear one, allows quick analysis and offers a high degree of accuracy, (GANCZ, V., and co., 2010).

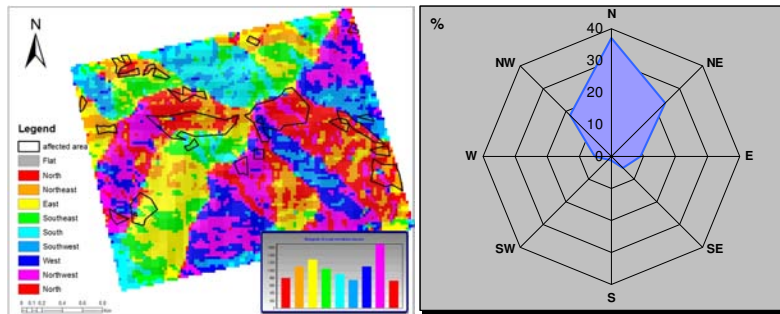


Fig. 3.6. Map slopes exposure for test area – (a); Affected area reported to slopes – (b).

The results acquired offer quantitative data, first about the exposure of the slopes. Exposure is an element of natural potential and has an important role in wind caused debris. Exposure can be used in various applications, in our case the exposure of the slopes affected by wind caused debris, figure 3.6(b) showing that they were mainly oriented towards north (37%), NE (24%) and NW (18%). Slopes with southern exposure were very little affected (S and SW 1%).

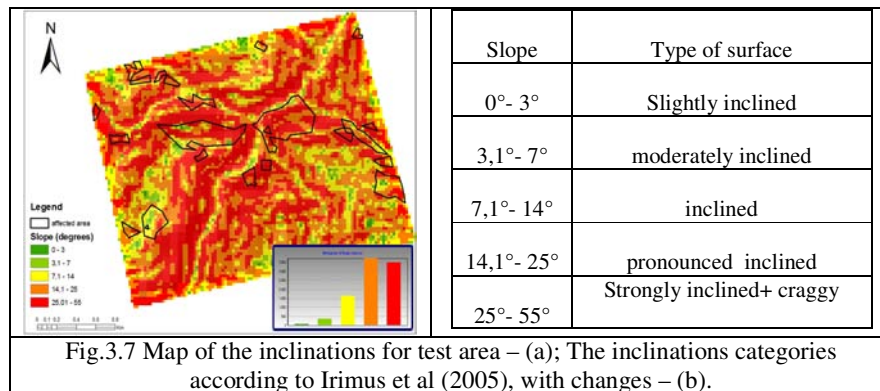


Fig.3.7 Map of the inclinations for test area – (a); The inclinations categories according to Irimus et al (2005), with changes – (b).

Besides slope exposure, another important factor is inclination. Inclination is understood as the size of altitude increasing with distance, in the direction where it is highest. The map of the inclinations is shown in figure 3.7, where they are expressed in degrees, classified in five scales and rendered in different colors.

Concerning the inclination categories utilized, these vary a lot, according to the objective for which they are analyzed. In order to determine the inclination categories which influence the windthrow, the categories suggested by Irimuş and co. (2005), but modified. (Figure 3.7-b)

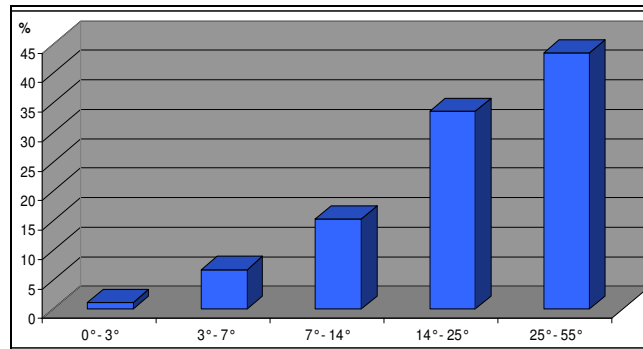


Fig. 3.8 Affected area by windthrow, reported to the slope

For the quantitative analysis, five classes of inclination were chosen and represented graphically (figure 3.8), therefore rendering the percentage values for each type of inclination. The windthrow was concentrated on the inclinations with values corresponding to superior classes. Therefore, the surfaces with an inclination between 25° to 55° were affected in proportion of 43%, but the surfaces with an inclination between 14° and 25° only 33%. Surfaces with an inclination between 0°-3° were the least affected, about 1%.

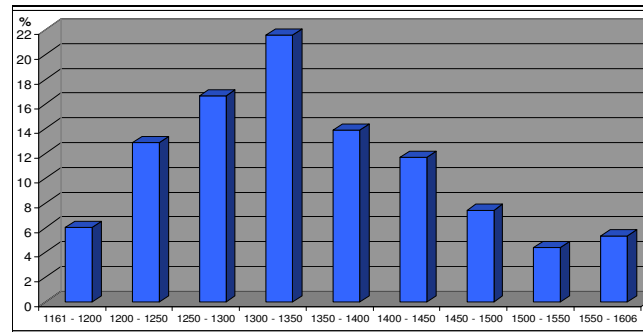


Fig. 3.9. Affected area by windthrow, reported to the altitude.

Another element with an important role in analyzing windthrow is altitude. To detail the altitude of the affected areas we defined 9 classes, between 1161m and

1606m. Thus it is observed that the most affected areas are those between 1300-1350m altitudes, with a percentage of 21.6%. A high percentage also has the area between 1250-1300m (16.7%), and the areas with altitudes between 1350-1400m (13.8%). The most affected areas are situated between 1200-1450m, with a percentage of 76.7% of the total.

Another stage of the research allows the evaluation of the effects in terms of affected areas, the results being presented graphically as well as in a chart. Figure 3.8 shows the classification in percentage of the affected areas according to surface, and attention is drawn to the fact that the highest percentage falls to the surfaces under 1 ha (43%)

In fig. 3.9 (b) the table generated in GIS for the affected areas ≥ 0.5 ha is presented. Here the area of the affected surfaces can be observed, the largest one being over 37ha.

Depending on the affected areas, the type of windthrow can be determined, classifying it as *endemic windthrow*, which group together the isolated debris and the ones in groups of 5-10 trees, as well as the type of mass debris, which affect a forest made of a certain species of trees, provided that this phenomenon – mass windthrow – is not generalized to a large geographical area.

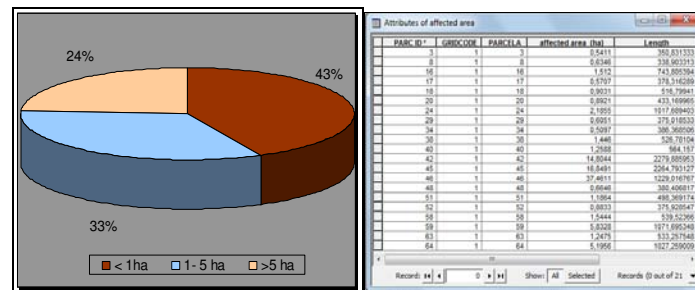


Fig. 3.10. The classification in percentage of the affected areas according to surface - (left), the table generated in GIS for the affected areas - (right).

Conclusions

This method for detecting the debris caused by wind with the help of satellite images allows a quick evaluation of the effects of the debris for a given area, on the grounds of the existing data in the database. The condition to a quick geo-spatial analysis is the existence of the landscape geo-spatial data in the affected areas, which can be exploited with the help of GIS software.

The geographical analysis allowed the highlighting of the way in which the morph-metric parameters influenced the debris, showing that the most affected were the slopes with northern exposure (37%), north-eastern and north-western.

The choosing of 5 classes of inclinations allowed the observation of the concentration of affected areas on the inclinations between 25°-55° (strong and steep inclination), with a percentage of 43% of the total.

The definition of the 9 classes of altitude between 1161m and 1606m allowed us the highlighting of the altitude for the affected areas. The most affected areas being between 1300-1350m, having 21.6%. In addition, it was observed that there was an uneven distribution in altitude, the most affected areas being between 1200m and 1450m, meaning 76.7%, and altitudes above 1450m represent 17%.

Another stage allowed us to determine the affected surfaces, performing a classification based on percentage of the areas affected according to the surface. The areas most affected by windthrow were under 1 ha (43%); the largest affected area having a little over 37ha.

References:

- Air Weather Service (AWS) (1996):** *Echoes: Operational use of vertically integrated liquid (VIL)*, No. 16. Scott AFB: Air Weather Service.
- Bogdan, Octavia, Coşconea, Maria, (2010),** *Riscul doborâturilor de arbori în România (Cauzele)*, Riscuri și Catastrofe, An.IX, vol.3, nr. 1/2010.
- European Sever Weather Database (2011):**
<http://essl.org/cgi-bin/eswd/eswd.cgi#lookupanchor>
- Gancz, V., et al., 2010,** *Detectarea cu ajutorul imaginilor satelitare a doborâturilor de vânt și evaluarea efectelor acestora*, Revista Padurilor, nr.6/2010.
- Irimus, I. A., et al., 2005,** *Tehnici de cartografiere, monitoring si analiza GIS*, Editura Casa Cartii de Stiinta, Cluj-Napoca
- Păuna, A. , (2011) ,** *Cercetări privind doborâturile de vânt și principalii factori biotici vătămători, în molidul din raza D.S Argeș*, Teză de doctorat.
- Popa, I., (2007),** *Managementul riscului la doborâturi produse de vânt*, Editura Tehnică Silvică, București.
- Popa I., (2005) -** *Doborâturile produse de vânt – factor de risc în ecosistemele forestiere montane*, Analele ICAS, 48 : 171-195
- Popa, I., (2005),** *Doborâturile produse de vânt în contextul modificărilor de mediu*, În: Giurgiu, V. (ed.): *Silvologie*, vol. IVA. Editura Academiei Române, 157-184
- Popa, I., (2000),** *Sisteme de cartare a zonelor de risc la doborâturi produse de vânt*. Revista pădurilor.4.
- Wakimoto R. M. (2001):** Convectively driven high wind events. Severe Convective Storms: *American Meteorological Society*, 28, 255-298.
- *** (1962, 2003),** *Amenajamentele Ocolului Silvic Cugir*, D.S. Alba.
<http://www.esrl.noaa.gov>
<http://glovis.usgs.gov/>